

FORMATION OF SOLAR MAGNETIC FLUX TUBES WITH KILOGAUSS FIELD STRENGTH INDUCED BY CONVECTIVE INSTABILITY

SHIN'ICHI NAGATA,¹ SAKU TSUNETA,² YOSHINORI SUEMATSU,² KIYOSHI ICHIMOTO,² YUKIO KATSUKAWA,²
 TOSHIFUMI SHIMIZU,³ TAKAAKI YOKOYAMA,⁴ THEODORE D. TARBELL,⁵ BRUCE W. LITES,⁶ RICHARD A. SHINE,⁵
 THOMAS E. BERGER,⁵ ALAN M. TITLE,⁵ LUIS R. BELLOT RUBIO,⁷ AND DAVID OROZCO SUÁREZ⁷

Received 2008 February 12; accepted 2008 March 6; published 2008 March 19

ABSTRACT

Convective instability has been a mechanism used to explain the formation of solar photospheric flux tubes with kG field strength. However, the turbulence of the Earth's atmosphere has prevented ground-based observers from examining the hypothesis with precise polarimetric measurement on the subarcsecond scale flux tubes. Here we discuss observational evidence of this scenario based on observations with the Solar Optical Telescope (SOT) aboard *Hinode*. The cooling of an equipartition field strength flux tube precedes a transient downflow reaching 6 km s^{-1} and the intensification of the field strength to 2 kG. These observations agree very well with the theoretical predictions.

Subject heading: Sun: photosphere

1. INTRODUCTION

The photospheric magnetic flux tubes with kG field strength and spatial scale of a few 100 km are ubiquitously found across the entire solar surface (Stenflo 1994). Those flux tubes appear as small bright points in the continuum and spectra lines (Keller 1992), and their dynamical properties have been well studied with filtergrams (for example, Title et al. 1989; Berger & Title 1996). On the other hand, their magnetic properties, which are studied in detail with precise spectropolarimetric measurements, have not been well understood. One of the fundamental problems in understanding these flux tubes is their formation.

Since they are frozen-in with the plasma, magnetic fields are swept into the intergranular downflow regions. Through this process known as flux expulsion, the field strength is increased to the limit roughly given by the equipartition of the magnetic energy density of flux tubes and the kinetic energy density of the granular flows (Parker 1963; Galloway & Weiss 1981). However, this equipartition field strength is typically $\sim 400 \text{ G}$; further intensification is necessary to explain the formation of kG field strength flux tubes.

The further intensification was independently suggested by Parker (1978), Spruit & Zweibel (1979), and Webb & Roberts (1978): convective instability of flux tubes with equipartition field strength can intensify the field strength up to a kG or more. The plasma in such flux tubes cools and falls due to the instability, and the flux tube narrows until the field strength is so strong that it can suppress the instability. The intensified field strength is given by balance between the magnetic pressure of the evacuated flux tube and the surrounding gas pressure, and the typical field strength is 1–2 kG. This process is referred to as convective collapse and has been studied in detail with

numerical simulations (Grossmann-Doerth et al. 1998; Steiner et al. 1998; Takeuchi 1999; Vögler et al. 2005).

Apart from possible examples of “aborted” convective collapse (Bellot Rubio et al. 2001; Socas-Navarro & Manso-Sainz 2005), no direct observational evidence for this model has been obtained so far. From the observational point of view, it is necessary to perform continuous and precise measurement of the magnetic fields of flux tubes to reveal their formation process. However, even with modern adaptive optics techniques, it is very difficult for ground-based instruments to continue precise magnetic field measurements on those small flux tubes for their evolution times of several minutes.

The Solar Optical Telescope (SOT; Tsuneta et al. 2008; Suematsu et al. 2008; Shimizu et al. 2008; Ichimoto et al. 2008) aboard *Hinode* (Kosugi et al. 2007) was developed to overcome the difficulties inherent in the ground-based observations by observing the Sun from space. The diffraction limited spatial resolution of $0.2''$ and the pointing stability of $0.01''$ of SOT enable us to investigate the evolution of magnetic flux tubes with unprecedented accuracy (Suematsu et al. 2008; Shimizu et al. 2008). We here report the formation of a magnetic flux tube with kG field strength revealed with the SOT Spectro-Polarimeter (SP; Lites et al. 2001a, 2001b).

2. OBSERVATIONS AND ANALYSIS

The data used in this study were taken from 06:08:42 to 07:05:14 (UT) on 2007 February 6 in a quiet region at disk center. Full Stokes profiles of two Fe I absorption lines sensitive to the Zeeman effect at 6301.5 and 6302.5 Å were obtained to investigate magnetic field evolution. Raster scans on a small area of $4'' \times 40''$ were performed with temporal cadence of 50 s and with no pixel binning. The pixel size of the SP is about $0.16''$, while its spatial resolution is about $0.3''$; the anticipated Strehl ratio of the SP is expected to be ~ 0.5 due to the finite slit width of $\sim 0.16''$ (Lites et al. 2008). The data were taken in the so-called dynamics mode in which the integration time at each slit position was 1.6 s. The statistical error for each Stokes profile measurements were determined by a Gaussian fit for the core of intensity distribution for all the points taken during this observation period. The standard deviation was found to be $\sim 1/580$ for four profiles.

¹ Hida Observatory, Kyoto University, Takayama, Gifu 506-1314, Japan.

² National Astronomical Observatory, Mitaka, Tokyo 181-8588, Japan.

³ Institute of Space and Astronautical Science, JAXA, Sagami-hara, Kanagawa 229-8510, Japan.

⁴ Department of Earth and Planetary Science, University of Tokyo, Bunkyo-ku, Tokyo 113-0033, Japan.

⁵ Lockheed Martin Solar and Astrophysics Laboratory, B/252, 3215 Hanover Street, Palo Alto, CA 94304.

⁶ High Altitude Observatory, NCAR, P.O. Box 3000, Boulder, CO 80307-3000.

⁷ Instituto de Astrofísica de Andalucía (CSIC), 18080 Granada, Spain.

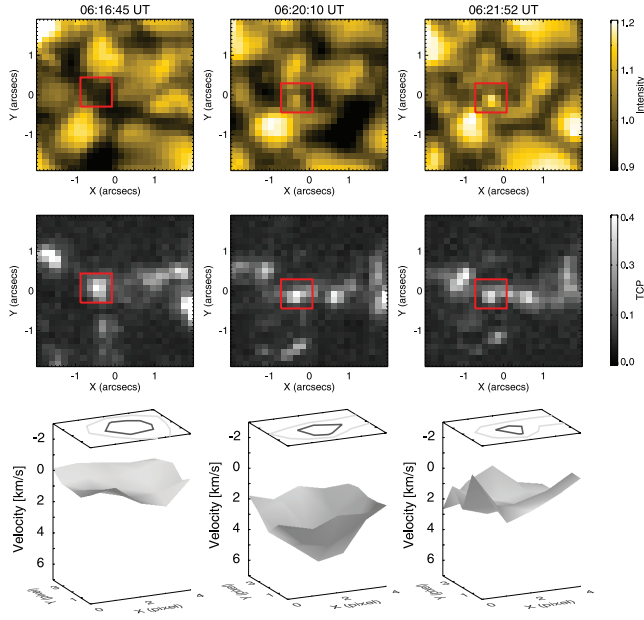


FIG. 1.—Formation of a kG field strength magnetic flux tube observed with SP. The three panels in the top row show the continuum intensity maps derived from the SP scan taken before, in the middle of, and after the formation of a kG field strength flux tube, from left to right, respectively. The red fiducial box of $0.8'' \times 0.8''$ (5×5 pixel²) in the maps encloses the intergranular lane where the evolving flux tube of interest is seen. The middle row shows the total circular polarization (TCP) of Fe I 6302.5. Each panel corresponds to the continuum maps shown above. The bottom row shows the line-of-sight velocity and the total circular polarization in the fiducial box shown in the upper rows. The surface plot shows the velocity distribution in the fiducial box; redshifted velocity is positive. Above the surface plots the contours of total circular polarization of 0.2 and 0.3 are shown with thin and thick lines, respectively.

We focus here on a part of a unipolar region with $4'' \times 4''$ area where a small magnetic feature with significant circular polarization signal was found. No significant linear polarization signals greater than the 3σ level were found there. Thus, we can assume that the observations represent the evolution of vertically oriented magnetic fields.

We examined the field strength, line-of-sight velocity, total circular polarization (TCP), and continuum intensity in this study. The field strength was derived through Milne-Eddington inversion for the two lines considering the magnetic filling factor. The TCP was derived by integration of the absolute value of the Stokes V profile of Fe I 6302. The integration range was for 6302.2–6303.0 Å; the lower limit was adjusted to avoid contamination from Fe I 6301. The line of sight velocity was derived from the Doppler shift of the Fe I 6302 Stokes V profile, where the shift was determined by the zero-crossing position of the V profile.

3. RESULTS

We show formation of a continuum bright point associated with transient strong downflow of the corresponding magnetic feature (Fig. 1). In the first column in Figure 1, no remarkable features are found in a fiducial box on the continuum map. On the other hand, a magnetic feature with strong circular polarization signal is found there. This magnetic feature does not show any significant velocities at this moment. In the second column in Figure 1, taken about 200 s later, a continuum bright point with ~ 1 pixel size in the middle of the fiducial box is clearly seen. Moreover, the magnetic feature corresponding to

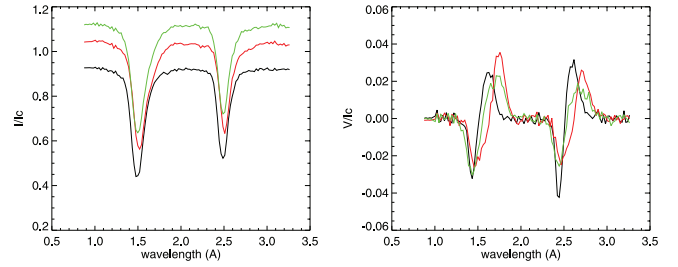


FIG. 2.—Left: Stokes I profiles observed at the central pixel of the growing bright point. The horizontal axis is the wavelength shift from 6300 Å. The black, red, and green lines represent the profiles observed in each column of Fig. 1 from left to right, respectively. Right: Stokes V profiles corresponding to the I profiles shown in the left panel. The colors of lines are the same as on the left. Note that all the profiles are normalized with the average continuum intensity.

the bright point shows a strong downflow with $\sim 6 \text{ km s}^{-1}$. In the last column of Figure 1, taken about 100 s after the second one, the continuum bright point becomes more prominent, whereas the strong downflow of the magnetic feature observed in the previous panel has ceased. See also the Stokes profiles emerging from the growing bright point (Fig. 2).

We next compare the evolution of field strength, line-of-sight velocity, and continuum intensity observed at the central pixel of the magnetic feature of interest (Fig. 3). We find a good coincidence between the evolution of field strength intensification and the downward motion. The initial field strength of $\sim 400 \text{ G}$ is intensified up to $\sim 2000 \text{ G}$ as the downflow grows to 6 km s^{-1} in 150 s. The field strength then remains above 1000 G throughout the sequence. We also find another characteristic of the velocity evolution, a transient upflow of $\sim 2 \text{ km s}^{-1}$ at the end of the sequence.

In contrast, the continuum intensity evolution looks different from that of the velocity and field strength. Continuum intensity gradually increases, and the peak intensity is reached after the maximum downflow velocity and after the field strength has reached its maximum. The continuum intensity variation can be interpreted as the temperature variation by assuming black-body radiation. By using the normalized continuum intensity observed before and after the appearance of the bright point, ~ 0.9 and ~ 1.1 respectively, and effective photospheric tem-

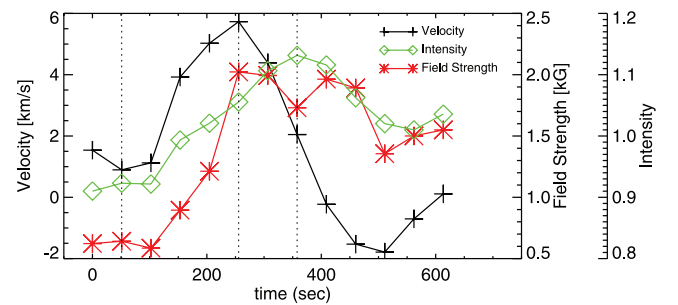


FIG. 3.—Evolution of the velocity, continuum intensity, and field strength observed at the center of the evolving flux tube. The physical parameters are extracted from the central pixel of the magnetic feature with a growing bright point. The black line with pluses represents the line-of-sight velocity derived from the Fe I 6302 Stokes V profile. The green line with diamonds represents the normalized field strength derived from the Milne-Eddington inversion for the observed profiles. Three dotted vertical lines represent the times when the scans shown in Fig. 1 were made. The start time is 2007 February 6 06:15:54 (UT).

perature of 5778 K, the temperature before and after the bright point formation is estimated to be 147 K lower and 140 K higher than the average temperature.

In addition to the field strength evolution, we also mention the magnetic flux evolution; magnetic flux is estimated with the field strength, filling factor, and spatial area. The magnetic flux in the pixel of interest increases during the field strength intensification, while the filling factor stays around ~ 0.5 ; this implies that magnetic flux is swept into the one resolution element. To investigate where the flux came from, we analyzed the magnetic flux evolution in a 5×5 pixel² box around the growing bright point. Magnetic flux there also increases during the field strength intensification. We thus suspect that magnetic flux in the vicinity of the box is swept into the downflow region, and are most densely condensed in the center, where a kG field strength flux tube appears. We exclude flux increase due to emergence, because emergence of flux with polarity opposite to that of the growing bright point is not found in the field of view shown in Figure 1 during the field strength intensification.

4. DISCUSSION AND CONCLUSION

The observed evolution of field strength, velocity, and temperature at a growing bright point with a magnetic feature is qualitatively consistent with the results of numerical simulations (Grossmann-Doerth et al. 1998; Steiner et al. 1998; Takeuchi 1999; Vögler et al. 2005). We interpret the observations as follows:

1. Due to thermal isolation from the surroundings by the magnetic fields, the radiative cooling of a flux tube drives convective intensification, which causes a strong downflow.
2. The field strength in the flux tube is intensified as the flux tube is evacuated with the downflow, keeping pressure balance with the surroundings.
3. The surface of unity optical depth goes down as the flux tube is evacuated, and the temperature at the surface is in-

creased by the radiation from the surroundings whose temperature is higher than that at the higher layer; the continuum intensity consequently increases (Spruit 1976).

4. The downward flow bounces back at the dense bottom layer, and the upward motion appears. Such “rebounds” have also been seen by Bellot Rubio et al. (2001) and by Socas-Navarro & Manso-Sainz (2005).

In the framework of the convective collapse picture it is clear that the continuum intensity reaches its maximum after the maximum of the downflow. As long as the downflow continues, the density in the upper part of the flux concentration continues to decrease, so that the level of optical depth unity sinks deeper and deeper. On the other hand, the magnetic field strength saturates at some point: when the plasma beta has become very small and the top is almost evacuated, the magnetic pressure is balanced by the external gas pressure and no further increase of the field strength is possible.

In conclusion, the observations are naturally explained with the convective collapse model; our observation provides strong support for the hypothesis that convective instability is an essential ingredient for kG flux tube formation.

Hinode is a Japanese mission developed and launched by ISAS/JAXA, with NAOJ as domestic partner and NASA and STFC (UK) as international partners. It is operated by these agencies in cooperation with ESA and NSC (Norway). This work was carried out at the NOAJ *Hinode* science center, which was supported by the Grant-in-Aid for Creative Scientific Research “The Basic Study of Space Weather Prediction” (head investigator: K. Shibata) from MEXT, Japan, a donation from Sun Microsystems, Inc., and NAOJ internal funding. The National Center for Atmospheric Research is sponsored by the National Science Foundation. This research was partially supported by Ministry of Education, Science, Sports, and Culture Grant-in-Aid for Young Scientists (B) 18740106 2006.

REFERENCES

- Bellot Rubio, R. L., et al. 2001, *ApJ*, 560, 1010
 Berger, T. E., & Title, A. M. 1996, *ApJ*, 463, 365
 Galloway, D. J., & Weiss, N. O. 1981, *ApJ*, 243, 945
 Grossmann-Doerth, U., Schüssler, M., & Steiner, O. 1998, *A&A*, 337, 928
 Ichimoto, K., et al. 2008, *Sol. Phys.*, in press
 Keller, C. U. 1992, *Nature*, 359, 307
 Kosugi, T., et al. 2007, *Sol. Phys.*, 243, 3
 Lites, B. W., Elmore, D. F., & Streander, K. V. 2001a, in *ASP Conf. Ser.* 236, *Advanced Solar Polarimetry: Theory, Observation, and Instrumentation*, ed. M. Sigwarth (San Francisco: ASP), 33
 Lites, B. W., et al. 2001b, *Proc. SPIE*, 4498, 73
 ———. 2008, *ApJ*, 672, 1237
 Parker, E. N. 1963, *ApJ*, 138, 552
 ———. 1978, *ApJ*, 221, 368
 Shimizu, T., et al. 2008, *Sol. Phys.*, in press
 Socas-Navarro, H., & Manso-Sainz, M. 2005, *ApJ*, 620, L71
 Spruit, H. C. 1976, *Sol. Phys.*, 50, 269
 Spruit, H. C., & Zweibel, E. G. 1979, *Sol. Phys.*, 62, 15
 Steiner, O., Grossmann-Doerth, U., Knoelker, M., & Schüssler, M. 1998, *ApJ*, 495, 468
 Stenflo, J. O. 1994, *Solar Magnetic Fields: Polarized Radiation Diagnostics* (Dordrecht: Kluwer)
 Suematsu, Y., et al. 2008, *Sol. Phys.*, in press
 Takeuchi, A. 1999, *ApJ*, 522, 518
 Title, A. M., et al. 1989, *ApJ*, 336, 475
 Tsuneta, S., et al. 2008, *Sol. Phys.*, in press
 Vögler, A., et al. 2005, *A&A*, 429, 335
 Webb, A. R., & Roberts, B. 1978, *Sol. Phys.*, 59, 249